Journal of Power Sources 192 (2009) 714–718

Contents lists available at ScienceDirect

Journal of Power Sources

journal homepage: www.elsevier.com/locate/jpowsour

Short communication

Decreasing the initial irreversible capacity loss by addition of cyclic sulfate as electrolyte additives

Atsushi Sano*, Satoshi Maruyama

TDK Corporation, Devices Development Center, 570-2 Matsugashita, Minamihatori, Narita-shi, Chiba 286-8588, Japan

ARTICLE INFO

Article history:
Received 18 February 2009
Received in revised form 20 February 2009
Accepted 23 February 2009
Available online 9 March 2009

Keywords:
Graphite
Cyclic sulfate
Irreversible capacity
SEI

ABSTRACT

Initial irreversible capacity loss in graphite electrodes was suppressed by 1,3,2-dioxathiolane-2,2-dioxide and its derivatives (cyclic sulfates) in propylene carbonate (PC) containing electrolyte. Cyclic voltammetry (CV) showed that cyclic sulfates were decomposed at higher potentials than that for electrolyte solvents. In galvanostatic charge and discharge measurement, first cycle efficiency was increased from 58.2% to 90.5% by the addition of 1,3,2-dioxathiolane-2,2-dioxide. Passivation films formed by cyclic sulfates were observed by X-ray photoelectron spectroscopy (XPS), FT-IR, and pyrolysis/GC/MS (pyro/GC/MS). These results indicate that the surface was covered by a PEO like polymer with the inner layer comprised of Li_2S like compounds.

1. Introduction

Graphite is used for the negative electrode of lithium-ion batteries. In the initial charging stage, electrolyte decomposition occurs because the potential of the graphite negative electrode is much lower than the potential of the decomposed electrolyte. The electrolyte decomposition products form a surface film which is called "Solid electrolyte interphase" (SEI) [1]. SEI prevents further electrolyte decomposition and enables the reversible charge/discharge cycle [2,3].

This electrolyte decomposition causes irreversible capacity. Irreversible capacity in the initial charging stage decreases the number of lithium-ions available in the cell and decreases the cell capacity. To achieve higher cell energy density, irreversible capacity loss must be decreased. Moreover, when a higher graphite surface area was used, the irreversible capacity was increased [4,5].

Inaba et al. observed the SEI growth on a negative graphite electrode at elevated temperature with an in situ atomic force microscopy (AFM) [6]. They concluded that solvent molecules penetrate the SEI and increase its thickness. The addition of vinylene carbonate suppressed the SEI growth and decreased the irreversible capacity [7]. Thus the SEI formed with some additives suppresses penetration through the SEI.

When propylene carbonate (PC) is used as the electrolyte solvent, PC is decomposed on the graphite negative electrode, accompanied by graphite exfoliation [8]. It is generally accepted that PC cannot form a protective film on the surface of a graphite electrode. However, PC is the preferable organic solvent, because of its high permittivity and low melting point. Many kinds of additives for PC have been suggested, especially vinyl compounds [9,10] and sulfite compounds [11,12]. Besenhard et al. reported on the effect of ethylene sulfite (ES) [12]. ES prevented PC decomposition and lithium-ion intercalated reversibly. Their work indicated that ES was decomposed at high potential and formed SEI on graphite before PC decomposition. Ota et al. [13,14] investigated the composition of the SEI formed by ES. They reported that the SEI mainly consisted of inorganic films like Li_2SO_3 and organic films like $ROSO_2Li$ based on XAFS and XPS measurements.

In this report, we investigated the additives which have high LUMO (lowest unoccupied molecular orbital) levels. Among them, we focused on cyclic sulfates that can form effective SEI on a graphite negative electrode. The effect of cyclic sulfate was investigated by means of cyclic voltammetry (CV), galvanostatic measurement, and the chemical constituents were analyzed by FT-IR, XPS and pyro/GC/MS.

2. Experimental

Artificial graphite powder (MCF: Meso phase carbon fiber) (Petoca materials) was mixed with poly vinylidene fluoride (PVdF) Kynar® 761A (Atofina) dissolved in N-methyl-2-pyrrolidone. The ratio of artificial graphite was 90 wt% and PVdF 10 wt%. The slurry of artificial graphite and PVdF was coated on copper foil (thickness: 17 μm) by doctor blade method. The coated sheet was dried and pressed. The sheet was cut into 15 mm in diameter and prepared as a negative electrode. Cyclic voltammetry was measured by a three-

* Corresponding author. Tel.: +81 476 37 1611x7628; fax: +81 476 37 1688.
E-mail address: sanoa@jp.tdk.com (A. Sano).

0378-7753/$ – see front matter © 2009 Elsevier B.V. All rights reserved.
doi:10.1016/j.jpowsour.2009.02.075

Table 1
Calculation results of LUMO for electrolyte solvents and additives.

	LUMO (eV)
PC	1.235
EC	1.175
DEC	1.255
ES	−0.329
DTD	0.006
MDTD	0.058
EDTD	0.063
PCS	−0.445

electrode cell. Lithium foil was used as the counter and reference electrode. Charge and discharge measurements were carried out with a two-electrode cell. The counter electrode was lithium foil of 100 μm thickness. The electrolyte solutions were 1 mol dm^{-3} $LiPF_6$ dissolved in PC or a mixture of ethylene carbonate (EC) and PC (1:1 by volume) (Ube Kosan). 1,3,2-Dioxathiolane-2,2-dioxide (DTD) (Aldrich) was mixed and dissolved at the rate of 5 wt% DTD in 1 M $LiPF_6$/PC or PC + EC (1:1).

The electrolyte of 4-methyl-1,3,2-dioxathiolane-2,2-dioxide (MDTD) and 4-ethyl-1,3,2-dioxathiolane-2,2-dioxide (EDTD) and phenyl cyclic sulfate (PCS) was synthesized by Asahi Kagaku. ES (Aldrich) was used without further purification.

XPS: The surface film on the negative graphite electrode was analyzed by X-ray photoelectron spectroscopy (XPS). The charged and discharged negative electrode was washed with dimethoxy ethane (DME) two times and vacuum dried. All operations were carried out under argon atmosphere to prevent exposure to moisture and air.

FT-IR: FT-IR was used to analyze the surface of the negative graphite electrode. The negative graphite electrode was charged and discharged and washed with diethyl carbonate. The electrode was measured under argon atmosphere.

Pyro/GC/MS: For measurement of pyrolysis/GC/MS (Pyro/GC/MS) the graphite electrode was prepared as follows. The charged and discharged graphite electrode was washed with DME and vacuum dried. The electrode was put into a glass tube under argon atmosphere and heated at 200 °C. Generated gas was trapped under −70 °C. The trapped gas was heated again at 240 °C and inlet to GC column. HP-innowax column was used.

3. Results and discussion

Calculation results of LUMO are shown in Table 1. The calculations were implemented in MOPAC version 7. The LUMO of cyclic sulfates is lower than that of solvents (PC, EC, DEC). Low LUMO compounds are easily reduced. This suggests that cyclic sulfates are reduced at a higher potential than PC. Yoshitake et al. [15] investigated the correlation between LUMOs and reduction potential of additives. They reported a roughly liner relation between LUMO and reduction potential. It appears that the cyclic sulfates decomposed at higher potential than PC form a surface film on the graphite electrode, and the surface films act as SEI.

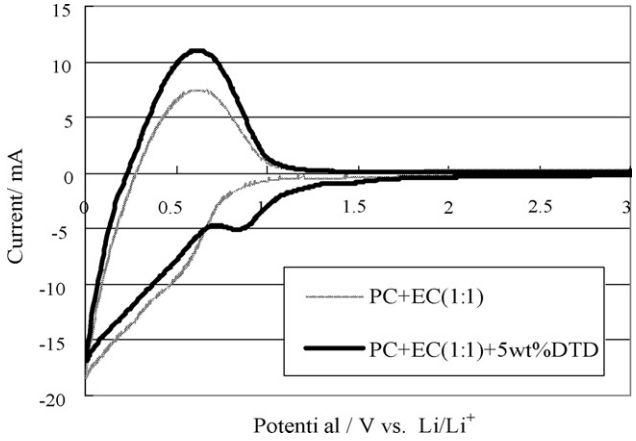

Fig. 1. Cyclic voltammograms of graphite (1st cycle) in (a) 1 M $LiPF_6$/PC + EC (1:1), (b) 1 M $LiPF_6$/PC + EC (1:1) + 5 wt% DTD. v = 5 mV/s.

PCS has the lowest LUMO among cyclic sulfates. Thus, calculation results indicate that cyclic sulfates are reduced at high potential and effectively form SEI. Actually the reduction potential cannot be estimated exclusively by LUMO. But calculation could be useful to screen compounds that can be used for additives.

Fig. 1 shows cyclic voltammograms of graphite in 1 M $LiPF_6$/PC + EC (1:1) and 1 M $LiPF_6$/PC + EC (1:1) + 5 wt% DTD. In 1 M $LiPF_6$/PC + EC (1:1), there is no significant peak until the potential sweeps from OCV to 1.0 V in the first cycle. Below 0.85 V, cathodic current of solvent decomposition was observed. In 1 M $LiPF_6$/PC + EC (1:1) + 5 wt% DTD, the reduction current is larger than for the 1 M $LiPF_6$/PC + EC (1:1) in the 2.0–1.5 V range. This shows that the reduction reaction in DTD added electrolyte was larger in the 2.0–1.5 V range.

Below 0.6 V, reduction current in the 1 M $LiPF_6$/PC + EC (1:1) + 5 wt% DTD is lower than that for the 1 M $LiPF_6$/PC + EC (1:1). This indicates that decomposed products of DTD formed an SEI on graphite and prevented PC decomposition. The anodic peak in 1 M $LiPF_6$/PC + EC (1:1) + 5 wt% DTD is larger than in 1 M $LiPF_6$/PC + EC (1:1). It is most likely that decomposed product of DTD prevented the graphite exfoliation accompanied with PC decomposition, and as a result, reversible capacity was increased, and anodic current was increased.

Fig. 2 shows the charge and discharge profile of graphite in 1 M $LiPF_6$/PC + EC (1:1). First cycle efficiency was 58.2%. The plateau observed below +0.85 V in first charging stage is the irreversible capacity ascribed to the decomposition of PC, which corresponds to the current peak below 0.6 V in CV measurement. 1 M $LiPF_6$/PC + EC

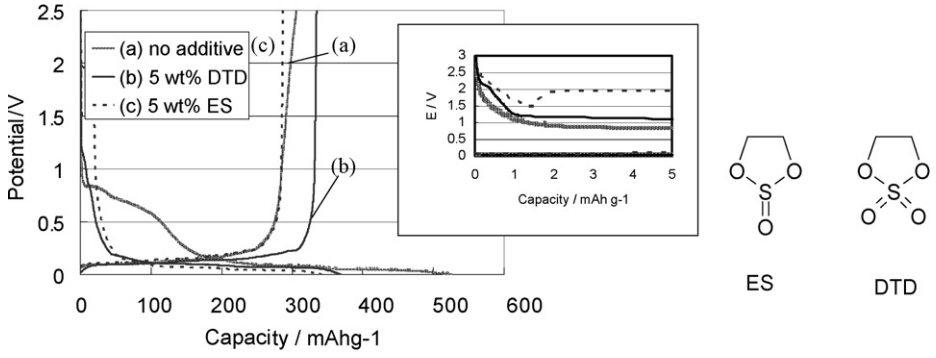

Fig. 2. First charge and discharge curves of MCF in (a) 1 M $LiPF_6$/PC + EC (1:1), (b) 1 M $LiPF_6$/PC + EC (1:1) + 5 wt% DTD, (c) 1 M $LiPF_6$/PC + EC (1:1) + 5 wt% ES.

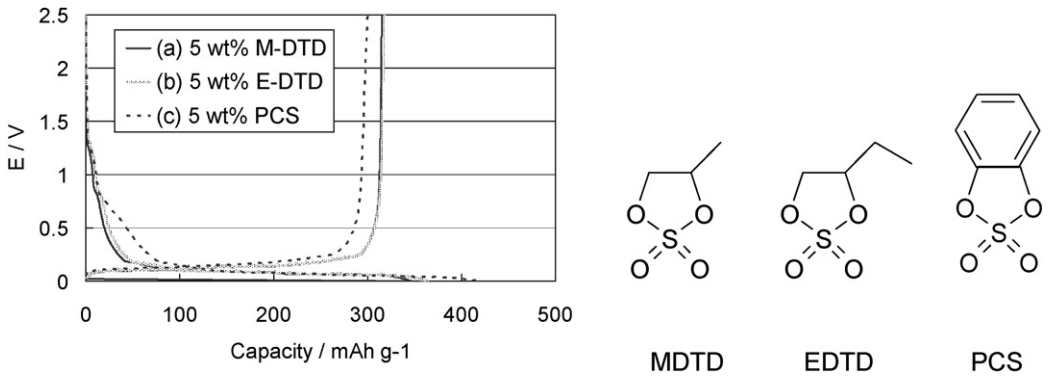

Fig. 3. Charge and discharge curves of MCF in first cycle in 1 M $LiPF_6$/PC + EC (1:1) (a) + 5 wt% M-DTD, (b) + 5 wt% E-DTD, (c) + 5 wt% PCS.

(1:1) formed SEI on graphite to some extent, but it was not sufficient to prevent PC decomposition completely.

Charge and discharge curves of graphite in 1 M $LiPF_6$/PC + EC (1:1) + 5 wt% DTD and 5 wt% ES are shown in Fig. 2. In 1 M $LiPF_6$/PC + EC (1:1) + 5 wt% DTD, the short plateau observed at 2.2 V would be DTD decomposition. Below 2.2 V, the potential dropped smoothly. Initial efficiency was 90.5%. In 1 M $LiPF_6$/PC + EC (1:1) + 5 wt% ES, the plateau corresponding to ES decomposition was observed at 2.0 V. First charge and discharge efficiency was 83.7%. Comparing DTD to ES, charge and discharge efficiency in DTD was better than in ES. The difference in efficiency is probably caused by the initial decomposition process. However, the amount of DTD is the same as for ES. The plateau in ES is much larger than that for DTD. This suggests that DTD formed SEI smoothly, and the SEI formed by DTD is highly protective against PC decomposition. Although LUMO of ES is lower than DTD, ES decomposed at lower potential than DTD. Thus decomposition potential and LUMO do not have a strictly liner relationship.

Fig. 3 shows charge and discharge curves of DTD derivatives. MDTD and EDTD is alkyl DTD and PCS. The profile of MDTD and EDTD almost overlapped. Initial efficiency of MDTD is 90.8% and for EDTD 87.4%. The efficiency of MDTD is almost the same as for DTD. The efficiency of EDTD is on the low side. This indicates that the long alkyl chain decreases the function of SEI. PCS has the lowest LUMO among cyclic sulfates. But the efficiency is quite low (71.7%). While MDTD and EDTD have alkyl chain and sulfate, PCS has phenyl

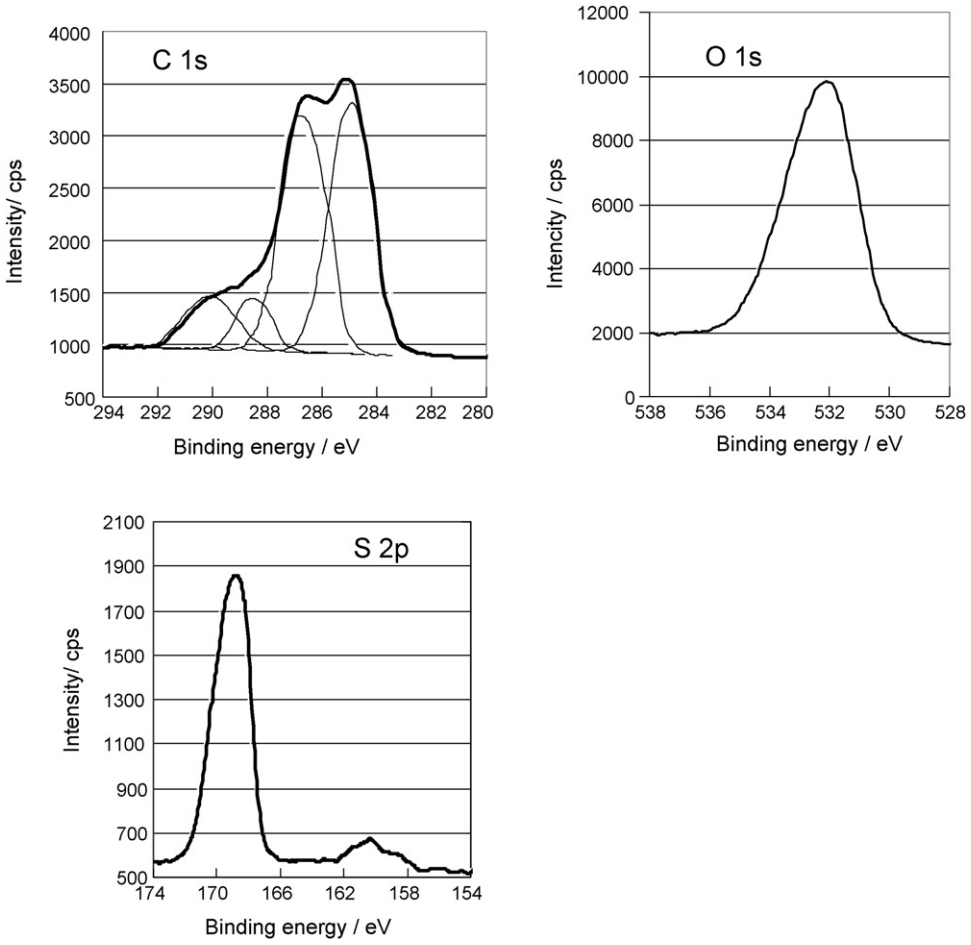

Fig. 4. XPS spectra of C 1s of the surface of MCF charged and discharged in 1 M $LiPF_6$/PC + EC (1:1) + 5 wt% DTD.

group. The effect of the alkyl chain is small, but the cyclic phenyl group has a significant effect. This result shows that the structure of the alkyl or cyclic phenyl group is more effective than that of the sulfate group. This is the important point in choosing the structure of additives.

XPS: Fig. 4 shows C 1s XPS spectra for the surface of the graphite electrode which was charged and discharged. Electrostatic charging observed in low conductivity materials provides a problem in determining the binding energy. Therefore the binding energy was determined by internal standards. The peak of aliphatic carbon (285.0 eV) was used as internal standard. The peak at 286.8 eV is assigned to CH_2CH_2O. C 1s spectrum of PEO corresponds to 286.5 eV [16]. Therefore the peak at 286.8 eV would be a PEO like compound. C 1s spectra at 288.6 eV corresponds to C(=O)O, which represents ester or carboxyl function [13]. The results of FT-IR indicate the presence of carboxyl function. Therefore the peak at 288.6 eV is assigned to carboxyl function. The peak at 290.1 eV corresponds to CO_3^{2-} derived from Li_2CO_3. From these results, C 1s spectra of the carbon surface indicates the existence of a PEO like polymer, and carboxyl salt and carbonate compounds.

O 1 s spectra show a peak at 532 eV. This peak corresponds to C=O (532.5 eV) or CO_3^{2-} (532 eV), which represent the $ROCO_2Li$ or Li_2CO_3 [17].

S 2p spectra at 169 eV is the peak of O–SO_2–O or SO_2– which is the decomposition products of DTD. S 2p spectrum at 169 eV in our analysis should be assigned to Li_2SO_3 or $ROSO_2Li$ [13,14]. The peak at 160 eV is reduced sulfur. It does not fit exactly to Li_2S, but it might be Li_2S, like reduced sulfur. After Ar^+ etching, the peak at 160 eV is increased compared to the peak at 169 eV. The intensity of C 1s spectra is decreased with Ar^+ etching except for the graphite peak. This suggests that the surface of SEI is composed of $ROCO_2Li$ and a PEO like polymer, while the inner layer is composed of reduced sulfur like Li_2S.

Sulfide compounds and PEO like polymers can act as solid state electrolytes. This suggests that the DTD decomposed products act effectively as SEI.

FT-IR: The results of FT-IR measurements are shown in Fig. 5. For no additives, a spectrum of $ROCO_2Li$ was observed at 1635 cm^{-1}, and 1570 cm^{-1} and is ascribed to Li_2CO_3. In DTD electrolyte, Li_2CO_3 is also observed. But $ROCO_2Li$ is absent or nearly so in DTD electrolyte. It has been reported that EC is decomposed to Li_2CO_3 and $ROCO_2Li$ [17,18]. The absence of $ROCO_2Li$ in DTD means that DTD decomposition products prevented the EC decomposition. SEI formed by DTD would prevent the EC decomposition as well as PC decomposition.

Pyro/GC/MS: Pyro/GC/MS analysis was carried out. Mass spectra represent the specific peak (m/z = 59, 103) in DTD. m/z = 59, 103 is

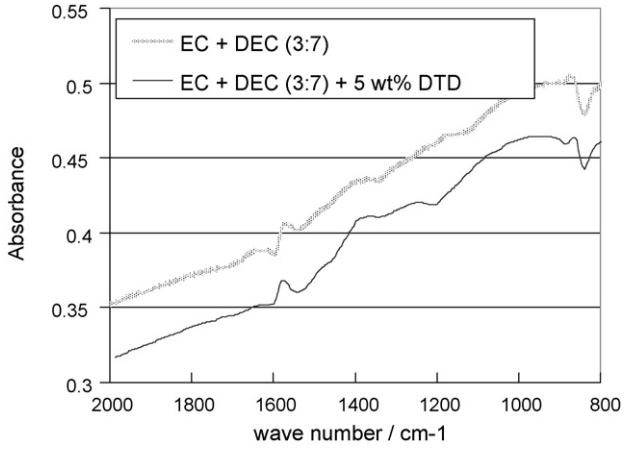

Fig. 5. FT-IR spectra of MCF charged and discharged in (a) 1 M $LiPF_6$/EC + DEC (3:7) + 5 wt% DTD, (b) 1 M $LiPF_6$/EC + DEC (3:7).

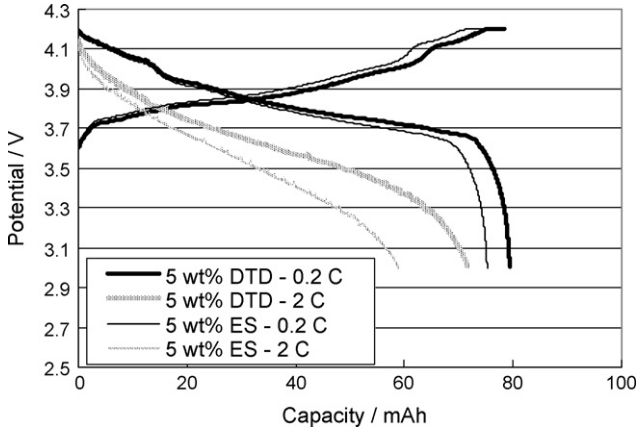

Fig. 6. Charge and discharge curves of cell in (a) 1 M $LiPF_6$/PC + EC (1:1) + 5 wt% DTD, (b) 1 M $LiPF_6$/PC + EC (1:1) + 5 wt% ES.

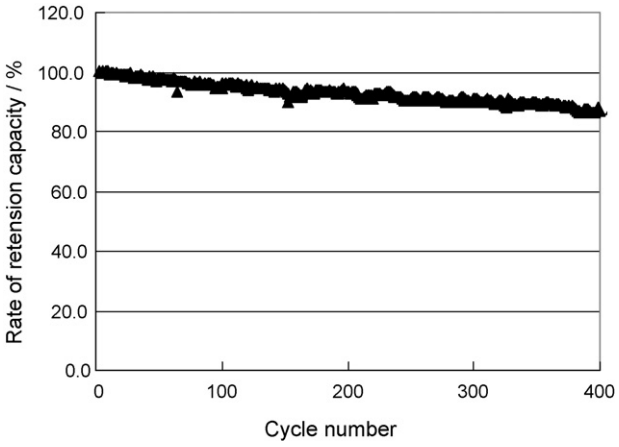

Fig. 7. Cycle ability of cell in 1 M $LiPF_6$/PC + EC (1:1) + 5 wt% DTD.

the fragmentation of ethylene oxide. The degree of polymerization is not identified. But the degree of polymerization would not be so high, n = 3–4, as in a previous report [19].

Cell performance of DTD is shown in Fig. 6. The cell with added DTD could charge and discharge at high efficiency. On the other hand, for no additives, it could not be charged because PC decomposed continuously. Fig. 7 shows the cycle ability of DTD. After 400 cycles, the capacity retention is 87%. This presents good cycle performance.

We suggest that O of DTD was reduced by 1 electron, to produce DTD anion radical. Subsequently DTD anion radicals react with other DTD at ethylene chain (Scheme 1). This process produces a PEO like polymer and Li_2SO_3. On the other hand, EC does not have LUMO probe at ethylene chain. Therefore it is most likely that the ethylene chain of DTD is attacked easier than that of EC and forms an effective SEI.

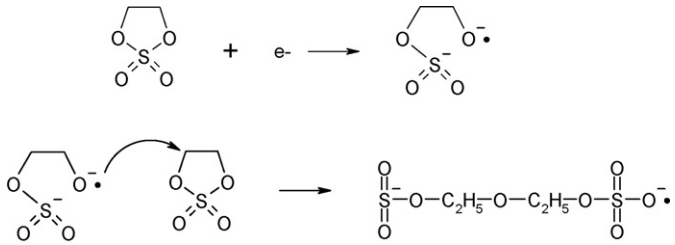

Scheme 1.

4. Conclusion

The effect of cyclic sulfate added to an electrolyte was investigated. DTD or DTD derivatives have low LUMO levels compared to electrolyte solvents such as PC or EC. SEI formed by DTD effectively prevented the PC decomposition on a graphite electrode. On the other hand, the lowest LUMO cyclic sulfate, PCS, had lower reversibility.

XPS measurement showed the presence of reduced sulfur. FT-IR measurement showed the absence of $ROCO_2Li$. Pyro/GC/MS measurement showed the presence of a PEO like polymer. The cell performance of DTD added electrolyte had a high efficiency and high cycle ability.

References

[1] E. Peled, J. Electrochem. Soc. 126 (1979) 2047.
[2] J.O. Besenhard, M. Winter, J. Yang, W. Biberacher, J. Power Sources 54 (1995) 228.
[3] Z. Ogumi, M. Inaba, Bull. Chem. Soc. Jpn. 71 (1998) 521.
[4] F. Chevallier, L. Aymard, J.-M. Tarascon, J. Electrochem. Soc. 148 (2001) A1216.
[5] T.S. Ong, H. Yang, J. Electrochem. Soc. 149 (2002) A1.
[6] M. Inaba, H. Tomiyasu, A. Tasaka, S.K. Jeong, Z. Ogumi, Langmuir 20 (2004) 1348.
[7] S.K. Jeong, M. Inaba, R. Mogi, Y. Iriyama, T. Abe, Z. Ogumi, Langmuir 17 (2001) 8281.
[8] A.N. Dey, B.P. Sullivan, J. Electrochem. Soc. 117 (1970) 222.
[9] K. Abe, H. Yoshitake, T. Kitakura, T. Hattori, H. Wang, M. Yoshio, Electrochim. Acta. 49 (2004) 4613.
[10] H.J. Santner, M. Winter, J.O. Besenhard, K.C. Moller, et al., Anal. Bioanal. Chem. 379 (2004) 266.
[11] G.H. Wrodnigg, J.O. Besenhard, M. Winter, J. Power Sources 97–98 (2001) 592.
[12] G.H. Wrodnigg, J.O. Besenhard, M. Winter, J. Electrochem. Soc. 146 (1999) 470.
[13] H. Ota, Y. Sakata, Y. Otake, K. Shima, M. Ue, J. Yamaki, J. Electrochem. Soc. 151 (2004) A1778.
[14] H. Ota, T. Akai, H. Namita, S. Yamaguchi, M. Nomura, J. Power Sources 119–121 (2003) 567.
[15] H. Yoshitake, K. Abe, T. Kitamura, J.B. Gong, Y.S. Lee, H. Nakamura, M. Yoshio, Chem. Lett. 32 (2003) 134.
[16] D. Briggs, G. Beamson, Anal. Chem. 64 (1992) 1729.
[17] D. Aurbach, Y. Ein-Eli, B. Markovsky, A. Zaban, J. Electrochem. Soc. 142 (1995) 2882.
[18] D. Aurbach, B. Markovsky, A. Shechter, Y. Ein-Eli, J. Electrochem. Soc. 143 (1996) 3809.
[19] Z. Ogumi, A. Sano, M. Inaba, T. Abe, J. Power Sources 97–98 (2001) 156.